A platform for Kirchhoff data mapping in scalar models of data acquisition

Norm Bleistein & Herman Jaramillo

ABSTRACT

Kirchhoff data mapping (KDM) is a procedure for transforming data from a given input source/receiver configuration and background earth model to data corresponding to a different output source/receiver configuration and background model. The generalization of NMO/DMO, datuming and offset continuation are three examples of KDM applications. This paper describes a "platform" for KDM for scalar wavefields. The word, platform, indicates that no calculations are carried out in this paper that would specialize the derived formula to any one of a list of KDM's that are presented in the text. Platform formulas are presented in 3D and in 2.5D. For the latter, the validity of the platform equation is verified by applying it to a Kirchhoff approximate representation of the upward scattered data from a single reflector and for an arbitrary source/receiver configuration. The KDM formalism is shown to map this Kirchhoff model data in the input source/receiver configuration to Kirchhoff data in the output source/receiver configuration, with one exception. The method does not map the reflection coefficient. Thus, we verify that, asymptotically, the ray theoretical geometrical spreading effects due to propagation and reflection (including reflector curvature) are mapped by this formalism, consistent with the input and output modeling parameters, while the input reflection coefficient is preserved. In this sense, this is a "true amplitude" formalism. As with earlier Kirchhoff inversion, a slight modification of the kernel of KDM provides alternative integral operators for estimating the specular angle, both in the input configuration and in the output configuration, thereby providing a basis for amplitude-versus-angle analysis of the data.

Glossary

$A(\boldsymbol{x}, \boldsymbol{x}_s(\boldsymbol{\xi}_O))$ A Green's function amplitude, with source at $\boldsymbol{x}_s(\boldsymbol{\xi}_O)$ and observation point at $\boldsymbol{x}$. Other choices, s replaced by g and/or O replaced by I. Equation (2).

$a_I(\boldsymbol{x}, \boldsymbol{\xi}_I),\ a_O(\boldsymbol{x}, \boldsymbol{\xi}_O)$ Amplitudes of modeling (O) and inversion. Equation (2). (I), operators, each a product of Green's function.

$\beta(\boldsymbol{x})$ The reflectivity function, product of a singular function of a surface and a reflection coefficient at a distinguished incidence angle. Equation (7).

$c(\boldsymbol{x})$ Wavespeed.

γ Variable in 2D coordinate system, varying along the isochron, $T_I \equiv \tau_I(\boldsymbol{x}^I(\gamma, T_I))$.

$\Delta\tau_I$ Difference of second derivatives of travel time in a stationary phase calculation. Equation (28).

$\delta(n_R)$ A Dirac delta function with argument being normal distance to a surface; the singular function of the surface.

$\mathcal{G}$ Shorthand for a collection of amplitude factors. Equation (21).

$H(\boldsymbol{x}, \boldsymbol{\xi}_I)$ The Beylkin determinant (2×2) that arises in two dimensional inversion. Equation (15).

$h(\boldsymbol{x}, \boldsymbol{\xi}_I)$ The Beylkin determinant (3×3) that arises in three dimensional inversion. Equation (9).

$\kappa_I,\ \kappa_O$ Curvatures of input and output isochrons, respectively.

$\omega_I,\ \omega_O$ Input, output frequencies, respectively.

$\hat{\boldsymbol{n}}_R$ Unit normal vector to the reflection surface.

$R(\boldsymbol{x}, \boldsymbol{x}_s)$ Geometrical optics reflection coefficient at $\boldsymbol{x}$ due to a source at $\boldsymbol{x}_s$.

$\sigma_{Is},\ \sigma_{Ig},\ \sigma_{Os},\ \sigma_{Og}$ Running parameters along the rays from source or receiver in the input or output configurations, respectively.

T_I Isochron coordinate of fixed input time in 2D: $T_I \equiv \tau_I(\boldsymbol{x}^I(\gamma, T_I))$.

$\tau_I(\boldsymbol{x}, \boldsymbol{\xi}_I),\ \tau_O(\boldsymbol{x}, \boldsymbol{\xi}_O)$ Travel time from source to point at depth to receiver in input or output source/receiver configuration, respectively.

θ_I, θ_O Half angles between rays from source and receiver to a point at depth in the input or output configuration, respectively.

$u_I(\boldsymbol{\xi}_I, \omega_I)$ Input data, observed data.

$u_O(\boldsymbol{\xi}_O, \omega_O)$ Output data, result of data mapping.

$\boldsymbol{x}^I(\gamma, T_I)$ Function defining the coordinate transformation from variables, $\boldsymbol{x}$ to variables, (γ, T_I) in 2D. Equations (10) and (16).

$\boldsymbol{x}_R(\ell)$ Function defining the reflector in 2.5D as a function of the parameter, ℓ.

$\boldsymbol{x}_s$, $\boldsymbol{x}_g$ Coordinates of source and geophone in input or output variables, depending on argument, $\boldsymbol{\xi}_I$, $\boldsymbol{\xi}_O$ respectively.

$\boldsymbol{\xi}_I$, $\boldsymbol{\xi}_O$ Input, output parameters used to define the source/receiver coordinates.

Introduction

"Kirchhoff data mapping" (KDM) is a process for transforming data from one prescribed source/receiver configuration and model of the propagating medium to another configuration and model. KDM is a "true amplitude" process in the following sense.

(i) Travel time and point source geometrical spreading effects of the input configuration are transformed to those effects of the output configuration.

(ii) Reflector curvature geometrical spreading effects of the input configuration are transformed to those effects of the output configuration.

However, the reflection coefficient of the input configuration is preserved in the output data. On the other hand, the formalism provides a mechanism for determining both the input and the output geometrical optics incidence angles of the reflection process in these applications, thereby providing a basis for amplitude-versus-angle (AVA) analysis. Both of these transformations are model consistent; that is, they depend on the input and output physical models that are assumed for the processing.

This research is grounded in the process of *transformation to zero offset* (TZO)—the true amplitude mapping of data from finite offset between source and receiver to zero offset. The constant background specialization of that technique is the *Normal MoveOut/Dip MoveOut* [NMO/DMO] method, which are standard tools in seismic data processing. The research was initially motivated by a desire to develop a specific technology and computer software for TZO in a depth-dependent earth model. That application will be reported on separately in Jaramillo [1998]. It extends the earlier NMO/DMO process in depth dependent background of Artley and Hale [1992] and Hale and Artley [1993] to a true amplitude process.

It became clear to us that the approach of Tygel, et al, [1997], as well as earlier papers, [Tygel, et al, 1995a, 1995b] had certain advantages over other approaches, including one of our own [Bleistein, et al, 1998]. However, we exploit an approximation of the obliquity factor in the Kirchhoff model that allows us to push the transformation process further than the results of the motivating papers. In a companion paper, Jaramillo and Bleistein [1997], the authors have derived a migration/demigration formalism in the space-time domain, based on the generalized Radon transform inversion technique. In Jaramillo [1998], that work is extended to a data mapping formalism in space-time. There, our obiliquity approximation is also exploited. Furthermore, Tygel, et al, [1998], did not mention the possibility of transforming the physical model, as suggested here. However, the necessary machinery to do so is available in their work.

The basic idea of these methods is to cascade an inversion formula with a modeling formula. The combined formula maps a given data set to another. Both of the operators used are integral operators. Thus, the result is an integral over the variables of the input data set—here denoted by $\boldsymbol{\xi}_I$ and ω_I—to produce an estimated model of a reflectivity in the subsurface combined with an integral over the coordinates of that model—here denoted by $\boldsymbol{x}$—to produce the output data set—with variables $\boldsymbol{\xi}_O$ and ω_O.* The input data set depends only on the variables of the acquisition geometry and time (or frequency)—the variables $\boldsymbol{\xi}_I$ and ω_I. The operator is a function of the input and output parameters and the reflectivity model variables, as well; that is, all of the variables introduced above. The idea, then, is to carry out the integration over (earth modeling) variables, $\boldsymbol{x}$, asymptotically, to obtain a weight that is a function of the input and output variables, only. This weight is then applied to the input data set to produce the output data set. It is this asymptotic analysis that can only be partially carried out in the absence of an explicit KDM implementation; hence, the word, "platform," to characterize this point of departure from which to derive the mapping of specific implementations.

Tygel et al [1998] and Jaramillo and Bleistein [1997] carry out this process in space-time, while a space-frequency derivation is presented here. An advantage of

* In this notation, the source and receiver coordinates are given parametrically as functions of the variables $\boldsymbol{\xi}_I$ and $\boldsymbol{\xi}_O$, respectively. By this device, specification of the source/receiver configurations is postponed to specific applications.

space-time methods is that the time domain integral produces a delta function that essentially reduces the dimension of the space-domain integration.† The equivalent process, in the approach here, is to decompose the volume integral into an integral along an isochron, a surface of constant travel time (We use isochrons of the input travel time.) followed by an integral over that travel time variable. This leads to an $n-1$ dimensional (1 or 2) integral followed by a one-dimensional integral. The iterated asymptotic analysis of this approach is easier than the approach of Bleistein, et al [1998], where an n dimensional stationary phase calculation is carried out. It also lends itself more easily to geometric (ray theoretical) interpretation.

The forward model used here, and in the companion Jaramillo and Bleistein [1997] paper, is a volume integral version of the *Kirchhoff approximation*. Tygel et al [1998] also start from a Kirchhoff approximation for the modeling of data, but as a surface integral. Cohen, et al, [1986] start from the Born approximation, which is also a volume integral. Thus, the issue of "small perturbations," as opposed to more general variations in medium parameters, arises in the Bleistein, et al [1998] approach. Although this assumption is overcome through further asymptotic analysis of the final result [Bleistein, 1987], it is certainly much cleaner to start from the Kirchhoff approximation. This is a single reflector model, requiring negligible errors in the earth model above the reflector of interest. It also neglects multiple reflections, as do all methods for data mapping (including classic DMO) to date. However, the approach used here *does* allow for larger jumps in medium parameters across the reflector of interest. Thus, in the absence of multi-pathing,‡ the interpretation of the output in terms of the geometrical optics reflection coefficient is direct and immediate in this approach, while the former approach of Bleistein, et al [1998] only predicts a linear approximation of the reflection coefficient in the output. It is only through *a posteriori* analysis that the Bleistein, et al [1998] approach confirms an output that is linear in the geometrical optics reflection coefficient [Bleistein, 1987].

The volume integral form of the Kirchhoff approximation requires introducton of the *singular function* of the reflecting surface. This is a Dirac delta function of normal distance from the reflector. For the inverse problem, it is necessary to isolate all dependence on the reflector in the *reflectivity function*, which is the singular function multiplied by the plane wave (or geometrical optics) specular reflection coefficient at a distinguished incidence angle. This isolation requires an asymptotic approximation for the *obliquity factor* appearing in the Kirchhoff representation and also requires that the reflection coefficient be evaluated at specularity. This is the new idea that we bring to the derivation of the basic inversion formula. Once that is done, a direct inversion procedure from the volume Kirchhoff-approximate forward model to an asymptotic inversion that produces the reflectivity function is carried out.

† This sequence is demonstrated in 2.5D KDM in the third section, below.

‡ Multi-pathing refers to the situation in which more than one ray path from a point at depth reaches the same point in the source receiver domain, either on input or output. Multi-pathing is neglected in the discussion in this paper.

KDM options.

Below, is a list some possible mappings of data sets from an input macro-model and source/receiver configuration to an alternative data set on output. All of these can be carried out in 2D, 2.5D and 3D.

(i) **Offset continuation and TZO.** KDM is not limited to transforming to zero-offset; the formula lends itself to analysis of the transformation of data from one offset to another, with TZO as a special case. That is, (10) and (16), below, provide a platform for *offset continuation* along the lines of Fomel [1995a,b, 1996, 1997] and Fomel et al [1996]. However, as soon as one applies to the platform equations the type of asymptotic analysis that leads to the classical NMO/DMO-type data mapping, the mapping requires "large" (e.g., a few wave lengths) offset to be valid.

(ii) **Transformation of common-offset data to common-shot data.** In this case, the transformed data represents the response from a single shot at an array of receivers covering the upper surface. Such data has the advantage that it is the solution of the wave equation, whereas common-offset (and zero-offset) data are a collection of single responses to an ensemble of wave equations, one for each shot. This ensemble data is not a solution of the wave equation, although it is treated as such in *wave equation migration.*

(iii) **Mapping of data from variable background propagation parameters to constant background parameters.** Time sections in constant background media are easier to interpret. It is not clear to us at this point, however, how multi-paths will map, nor how data from vertical and overhung reflectors will map. We expect singularities of the mapping process for these cases. On the other hand, where the method works, it opens the mapped data set to a much broader suite of applicable migration/inversion programs and related analysis techniques.

(iv) **"Unconverting" mode-converted waves.** For example, one could map the scalar components of

P-SV data to the scalar components of P-P data [Chan and Stewart, 1996]. If the "true" P-P data were available, a comparison of this latter data set with the mapped data set could provide a check on the assumptions made in the macro-model for the converted wave propagation. Furthermore, again, there are many more processing options available for P-P data than for mode converted data. This mapping would provide a means of extending the range of processing options once the data is mapped.

(v) **Velocity analysis.** When data from a suite of offsets are all mapped to zero offset, events should line up. To the extent that they do not, they provide the same type of information about velocity errors as does a common trace gather of a suite of prestack migrations/inversions.

(vi) **Wave equation datuming.** The acquisition surface can be changed for both the sources and receivers. Downward continuation of sources and receivers or mapping from irregular acquisition topography to a planar topography, are two potential datuming applications for this platform. See Sheaffer and Bleistein [1998]. For small increments in depth, the implementation of KDM provides an alternative to phase shift migration [Gazdag and Squazzero, 1984], while for larger increments in depth, the implementation of KDM provides an alternative to wave equation datuming [Berryhill, 1979].

(vii) **Mapping of swath data to a single line at zero azimuth.** Swath shooting is a process whereby multiple lines of receivers are used with a single shot, as might occur if a boat towed more than one sonophone line. The data from the separate lines could be mapped to a single line that could be "straightened" to be along the line of the survey—given sufficient information about the deviation of the swath survey from that line and about the path of the boat [Biondi and Chemingui, 1994].

(viii) **Combinations of the above.** For example, consider the application of downward continuation of receivers (or sources). The continuation process always yields output data over a shorter line than that of the input data. Starting from a prescribed shot gather with a given cable length of receivers, the cable length of asymptotically accurate mapped data decreases from the input cable length with increasing depth. On the other hand, consider first creating a single common shot data set from the full array of common offset gathers. This new data set effectively has a "cable length" equal to the length of the survey, typically, much longer than the cable length for each shot. Now, the range of validity of the downward continuation of receivers "shrinks" from an initial length equal to the survey length. One can expect that the data can be continued much deeper into the subsurface and maintain properly transformed geometrical spreading effects and travel time corrections over a cable length that will be adequate for further processing. As a second example of cascading, consider the process of first downward continuing the receivers and then downward continuing the sources. This should provide a true amplitude simultaneuos downward continuation of sources and receivers.

This paper proceeds as follows. In the next section, the fundamental three dimensional KDM platform equation is derived. The restrictions are that this is a platform for scalar data acquisition, no multiple reflections and no multi-pathing of rays from points at depth to either the input or output acquisition surface. Following that, the specialization to 2.5D processing is discussed. The result is a KDM platform for processing a line of data while honoring 3D propagation.

Then, a simple proof of the validity of the 2.5D data acquisition platform formula is presented. Under the restrictions stated above, this proof is carried out in all of the generality of the mapping formulation. The proof is valid for synclinal reflectors that might produce buried foci; their multiple arrivals do not cause a problem in this method. The exclusion of multi-pathing, applies only to structure sufficiently complex that the rays of the Green's function have multiple paths from a point at depth to a point on the upper surface.

Derivation of a 3D Kirchhoff data mapping formula

In this section, the fundamental equation for space-frequency domain KDM in 3D will be derived. This will be done by cascading a Kirchhoff-approximate forward modeling formula with an inversion formula. Crucial to this analysis is the representation of the Kirchhoff modeling formula as a volume integral in which the only unknown from the point of view of the inverse problem will be the reflectivity function described in the introduction. The derivation starts with the Kirchhoff approximation for the upward scattered wave from a single reflector. This representation can be found in many sources; we use equation (5.3.1) in Bleistein, et al [1997].

$$u_O(\boldsymbol{\xi}_O,\omega_O) \sim i\omega_O F(\omega_O)\int_{S_R} a_O(\boldsymbol{x},\boldsymbol{\xi}_O) \cdot\hat{\boldsymbol{n}}_R\cdot\nabla_x\tau_O(\boldsymbol{x},\boldsymbol{\xi}_O)\, R(\boldsymbol{x},\boldsymbol{x}_s) \cdot e^{i\omega_O\tau_O(\boldsymbol{x},\boldsymbol{\xi}_O)}dS_R. \tag{1}$$

In this equation, the subscript O is used to denote output variables. Later, input variables with subscript I will be introduced. The two component vector, $\boldsymbol{\xi}_O$, is used to parametrize the source and receiver locations, $\boldsymbol{x}_s(\xi_O)$ and $\boldsymbol{x}_g(\xi_O)$, respectively, and ω_O denotes the frequency of the output wave. The upward unit normal to the reflecting surface, S_R is denoted by $\hat{\boldsymbol{n}}_R$. The phase and amplitude are given by

$$\tau_O(\boldsymbol{x},\boldsymbol{\xi}_O) = \tau(\boldsymbol{x},\boldsymbol{x}_s(\boldsymbol{\xi}_O)) + \tau(\boldsymbol{x},\boldsymbol{x}_g(\boldsymbol{\xi}_O));$$
$$a_O(\boldsymbol{x},\boldsymbol{\xi}_O) = A(\boldsymbol{x},\boldsymbol{x}_s(\boldsymbol{\xi}_O)) \cdot A(\boldsymbol{x},\boldsymbol{x}_g(\boldsymbol{\xi}_O)), \tag{2}$$

with the separate traveltimes and phases being solutions of appropriate eikonal and transport equations, respectively, with initial point, $\boldsymbol{x}_s$ or $\boldsymbol{x}_g$, and final point, $\boldsymbol{x}$. We choose not to be more specific here, allowing for different propagations speeds in the eikonal equations (mode conversion) and transport equations appropriate to the degree of generality of the propagation model under consideration. The amplitudes can also include products of transmission coefficients arising from interfaces above the surface, S_R.

It should be noted that, except for the obliquity factor, $\hat{\boldsymbol{n}}_R \cdot \nabla_x \tau_O(\boldsymbol{x},\boldsymbol{\xi}_O)$, and the reflection coefficient, $R(\boldsymbol{x},\boldsymbol{x}_s)$, the elements of the integrand are defined globally in $\boldsymbol{x}$ and not just on the reflecting surface. That restricted dependence will be isolated further, to R, alone, in order to derived an inversion formula. Thus, what is needed is an approximation of the factor, $\hat{\boldsymbol{n}}_R \cdot \nabla_x \tau_O(\boldsymbol{x},\boldsymbol{\xi}_O)$ that is independent of surface information, that is, independent of $\hat{\boldsymbol{n}}_R$. The right choice here is the stationary value of this factor; at the stationary point(s) of the original surface integral, (1),

$$\hat{\boldsymbol{n}}_R \cdot \nabla_x \tau_O(\boldsymbol{x},\boldsymbol{\xi}_O) = -|\nabla_x \tau_O(\boldsymbol{x},\boldsymbol{\xi}_O)|. \tag{3}$$

The right side, here, is independent of the coordinates of the reflecting surface and, so, this approximation is substituted into (1). This is consistent with the intent of deriving an inversion for the reflectivity function, only. It acknowledges that high frequency modeling and inversion uses reflection data to detect reflecting surfaces. With this approximation, (1) is rewritten as

$$u_O(\boldsymbol{\xi}_O,\omega_O) = -i\omega_O F(\omega_O)\int_{S_R} a_O(\boldsymbol{x},\boldsymbol{\xi}_O) \cdot|\nabla_x \tau_O(\boldsymbol{x},\boldsymbol{\xi}_O)| R(\boldsymbol{x},\boldsymbol{x}_s) \cdot e^{i\omega_O \tau_O(\boldsymbol{x},\boldsymbol{\xi}_O)} dS_R. \tag{4}$$

The next goal is to rewrite the integral in (4) as a volume integral by introducing the *singular function of the reflecting surface*, $\delta(n_R)$, where n_R measures normal distance from any point on the reflector. The new representation becomes

$$u_O(\boldsymbol{\xi}_O,\omega_O) \sim -i\omega_O F(\omega_O)\int a_O(\boldsymbol{x},\boldsymbol{\xi}_O) \cdot|\nabla_x \tau_O(\boldsymbol{x},\boldsymbol{\xi}_O)| \cdot R(\boldsymbol{x},\boldsymbol{x}_s) \cdot\delta(n_R) e^{i\omega_O \tau_O(\boldsymbol{x},\boldsymbol{\xi}_O)} dV \tag{5}$$

Here, $dS_R dn_R = dV$. At worst, a reasonable continuation of the reflection coefficient off the reflecting surface must be introduced in this equation. Of course, that continuation need only correspond to the true R on the support of the singular function, that is, on the reflector. Even for bandlimited delta functions, this is easy to achieve.

Just as the normal derivative of the travel time has been replaced by its stationary value, the reflection coefficient is replaced by its stationary value, as well. Then, the product, $R\delta$, appearing in this equation is just the *reflectivity function*, $\beta(\boldsymbol{x})$, of the Bleistein/Cohen inversion theory [Bleistein, et al, 1997, eq. 5.1.21]. In this case, (5) can be rewritten as

$$u_O(\boldsymbol{\xi}_O,\omega_O) \sim -i\omega_O F(\omega_O)\int a_O(\boldsymbol{x},\boldsymbol{\xi}_O) \cdot|\nabla_x \tau_O(\boldsymbol{x},\boldsymbol{\xi}_O)|\beta(\boldsymbol{x}) e^{i\omega_O \tau_O(\boldsymbol{x},\boldsymbol{\xi}_O)} dV \tag{6}$$

Side remark

This volume integral representation of Kirchhoff-approximate forward modeling could be used to derive an inversion formula for β, following the generalized Radon transform method introduced by Belykin [1985] for this problem or by the asymptotic Fourier approach in Bleistein, et al [1997]. Such a derivation would have the advantage of not assuming small perturbations in medium parameters across the reflector, although it would assume primaries-only propagation above the reflector, an accurate background model ("macro-model") above the reflector, and no multi-pathing.

The derivation of an inversion formula would then follow along the lines used for inverting the volume integral forward model of Born-approximate data, but without the added small perturbation constraints of that model. Of course, the inversion formula that would then be derived is exactly the formula for β. Rather than rederiving that formula, we need only identify the corresponding constituents of the forward modeling formula for α, equation (5.1.7) in Bleistein, et al, [1997], and use this correspondence to deduce the inversion formula for β from the inversion formula (5.1.19) for α, in Bleistein, et al, [1997]

The correspondence of elements is as follows, with constituents of (5.1.7) appearing on the left and constituents of (5) appearing on the right.

$$\omega^2 F(\omega) \iff -i\omega F(\omega)$$

$$\frac{a(\boldsymbol{x},\boldsymbol{\xi})}{c^2(\boldsymbol{x})} \iff a_O(\boldsymbol{x},\boldsymbol{\xi}_O)|\nabla_x \tau_O(\boldsymbol{x},\boldsymbol{\xi}_O)|$$

$$\alpha(\boldsymbol{x}) \iff R(\boldsymbol{x},\boldsymbol{x}_s)\delta(n_R)$$

Written in a set of variables consistent with this discussion, the reflectivity function is given by

$$\beta(\boldsymbol{x}) = \frac{1}{8\pi^3}\int d^2\xi_I \frac{|h(\boldsymbol{x},\boldsymbol{\xi}_I)|}{a_I(\boldsymbol{x},\boldsymbol{\xi}_I)|\nabla_x \tau_I(\boldsymbol{x},\boldsymbol{\xi}_I)|} \cdot \int i\omega_I \, d\omega_I \, e^{-i\omega_I \tau_I(\boldsymbol{x},\boldsymbol{\xi}_I)} u_I(\boldsymbol{\xi}_I,\omega_I). \tag{7}$$

In this equation, the subscript I is used to denote input variables (i.e., the original variables). The two component vector, $\boldsymbol{\xi}_I$, is used to parametrize the source and receiver of the input data, $\boldsymbol{y}_s(\boldsymbol{\xi}_I)$ and $\boldsymbol{y}_g(\boldsymbol{\xi}_I)$, respectively, and ω_I denotes the frequency of the input wave. The phase and amplitude are given by

$$\tau_I(\boldsymbol{x},\boldsymbol{\xi}_I) = \tau(\boldsymbol{x},\boldsymbol{y}_s(\boldsymbol{\xi}_I)) + \tau(\boldsymbol{x},\boldsymbol{y}_g(\boldsymbol{\xi}_I));$$
$$a_I(\boldsymbol{x},\boldsymbol{\xi}_I) = A(\boldsymbol{x},\boldsymbol{y}_s(\boldsymbol{\xi}_I)) \cdot A(\boldsymbol{x},\boldsymbol{y}_g(\boldsymbol{\xi}_I)). \tag{8}$$

The traveltimes and amplitudes are again solutions of the eikonal and transport equations, except that now the initial points will be chosen from $\boldsymbol{y}_s(\boldsymbol{\xi}_I)$ and $\boldsymbol{y}_g(\boldsymbol{\xi}_I)$. Furthermore,

$$h(\boldsymbol{x},\boldsymbol{\xi}_I) = \det \begin{bmatrix} \nabla_x \tau(\boldsymbol{x},\boldsymbol{\xi}_I) \\ \frac{\partial}{\partial \xi_{I1}} \nabla_x \tau(\boldsymbol{x},\boldsymbol{\xi}_I) \\ \frac{\partial}{\partial \xi_{I2}} \nabla_x \tau(\boldsymbol{x},\boldsymbol{\xi}_I) \end{bmatrix} \tag{9}$$

is the Beylkin [1985] determinant.

Equation (7) is an inversion formula for β derived directly from a Kirchhoff-approximate forward model for a single reflector. Here, however, we have another objective. We wish to the map an input data set, with its source/receiver configuration and background parameters (macro-model) to an output data set, with its source/receiver configuration and background parameters. Thus, the different subscripts, I and O on the variables. To achieve this, the representation (7) is substituted into (6) to obtain the following representation for the mapping of data from any input source/receiver configuration and background model to any output source/receiver configuration and background model:

$$u_O(\boldsymbol{\xi}_O,\omega_O) \sim -\frac{i\omega_O}{8\pi^3}\int i\omega_I \, d\omega_I \, d^2\xi_I \, u_I(\boldsymbol{\xi}_I,\omega_I) \cdot \int \frac{a_O(\boldsymbol{x},\boldsymbol{\xi}_O)}{a_I(\boldsymbol{x},\boldsymbol{\xi}_I)} \frac{|\nabla_x \tau_O(\boldsymbol{x},\boldsymbol{\xi}_O)|}{|\nabla_x \tau_I(\boldsymbol{x},\boldsymbol{\xi}_I)|} |h(\boldsymbol{x},\boldsymbol{\xi}_I)| \cdot e^{[i\omega_O \tau_O(\boldsymbol{x},\boldsymbol{\xi}_O) - i\omega_I \tau_I(\boldsymbol{x},\boldsymbol{\xi}_I)]} dV \tag{10}$$

Note that only the first line on the right side in this equations depends on the input data. The integration over the interior volume in the second and third lines depends on the modeling and inversion parameters, and not on the data. Hence, for each choice of input and output earth model and each choice of input and output source/receiver configuration, the integrations indicated in the second and third lines could be carried out to obtain an operator kernel that is a function of $\boldsymbol{\xi}_I$, ω_I, $\boldsymbol{\xi}_O$, and ω_O. Indeed, we anticipate carrying out those integrations by analytical methods including asymptotic methods such as multi-dimensional stationary phase. Numerical integration is out of the question. There are $O(n^3)$ coordinates of integration, with $O(n^3)$ input variables and $O(n^3)$ output variables. Clearly, the n's are different, but this is still an intractably large set of variables. The processing of this formula would require an integration over$O(n^3)$ variables to produce a function of $O(n^6)$ variables. A better choice is the analysis of the volume integral represented by the second and third line to obtain an analytically explicit kernel that depends only on the input and output variables, $\boldsymbol{\xi}_I$, ω_I, $\boldsymbol{\xi}_O$, and ω_O,.

From the derivation and the specific example of 2.5D DMO, it is expected that the result will not transform the reflection coefficient of the input data configuration to the reflection coefficient of the output configuration. However, we do anticipate that the geometrical spreading effects and curvature effects of the input configuration will be transformed to the correct effects for the output configuration. In fact, this has been proven by Tygel, et al, [1998], using a somewhat different approach to the same problem. While their proof does not include all of the cases listed above, it could easily be extended to them. In that sense, we consider their proof as all encompassing for this operator. However, a simpler, more straightforward proof is offered, below, for the general 2.5D KDM.

Spatial structure of the operator.

There is a certain amount of symmetry in the spatial structure of the operator that could have predicted in advance. The geometrical spreading of the input data is "undone" by the division by a_I, while the geometrical spreading of the output is introduced through the multiplication by a_O. Similarly, the obliquity effects in the input data are undone by the division by a gradient of the input travel time, while the obliquity effects of the output data are reintroduced by the gradient in the numerator. The arrival time of the input data manifests itself through the phase in the frequency domain. That is undone by the multiplication by the negative of the input traveltime multiplied by the input frequency in the phase of the operator. Similarly, the positive product of output frequency and output travel time in the phase of the operator introduces the "correct" arrival time on output. All of these variables are evaluated at stationarity of the integrand. In the simplest of such evaluations, the Hessian, the determinant of the matrix of second derivatives, evaluated at the stationary point will correct for curvature effects from input to output data.

The only unexplained factor, then, is the Beylkin determinant h, which does not lend itself to the same type of symmetry arguments. As in the inversion integral, (7), this is the factor that cannot be predicted from migration arguments. Here, we refer to Beylkin's [1985] original paper introducing this type of inversion and earlier work by Bojarski [1967, 1968, 1982] and by the first author and associates [Bleistein, 1975, 1976; Mager and Bleistein, 1978; Bleistein and Cohen, 1979] on physical optics far field inverse scattering. Analysis of the forward model, (2), suggests that the model data is proportional to a Fourier transform of the function, $R\delta$. However, the output variables are not a wave vector, $\boldsymbol{k}$, but a combination, $\boldsymbol{\xi}$, ω.

Similarly, then, in (7), the inversion is asymptotically a Fourier inversion with respect to some wave vector, $\boldsymbol{k}$, although the integration is over variables, $\boldsymbol{\xi}_I$ and ω_I. In the earlier work by Bojarski and by Bleistein and associates on far field inverse scattering, the relationship between the phase and a wave vector is explicit. When the far field approximation cannot be used, the choice is less obvious.

Beylkin has shown us that for the case of interest here, the correct relationship is that the wave vector is locally defined for each choice of $\boldsymbol{x}$, $\boldsymbol{\xi}_I$ and ω_I by the relationship,

$$\boldsymbol{k} = \omega_I \nabla_x \tau_I(\boldsymbol{x}, \boldsymbol{\xi}_I).$$

Thus, in (7) and in (10) the factor of h arises through the identity

$$dk^3 = \left|\frac{\partial(\boldsymbol{k})}{\partial(\boldsymbol{\xi}, \omega_I)}\right| d^2\xi_I d\omega_I = \omega_I^2 \left|h(\boldsymbol{x}, \boldsymbol{\xi}_I) d^2\xi_I d\omega_I.\right|$$

In fact, if h in (10) is replaced by the Jacobian appearing on the right side of this equation, then the remaining frequency dependence of the operator becomes ω_O/ω_I and has the same quotient symmetry and explanation as the spatial factors discussed above. That is,

$$u_O(\boldsymbol{\xi}_O, \omega_O) \sim -\frac{1}{8\pi^3}\int \frac{\omega_O}{\omega_I} u_I(\boldsymbol{\xi}_I, \omega_I) d^3k$$
$$\cdot \int \frac{a_O(\boldsymbol{x}, \boldsymbol{\xi}_O)}{a_I(\boldsymbol{x}, \boldsymbol{\xi}_I)} \frac{|\nabla_x \tau_O(\boldsymbol{x}, \boldsymbol{\xi}_O)|}{|\nabla_x \tau_I(\boldsymbol{x}, \boldsymbol{\xi}_I)|} \tag{11}$$
$$\cdot e^{[i\omega_O \tau_O(\boldsymbol{x}, \boldsymbol{\xi}_O) - i\omega_I \tau_I(\boldsymbol{x}, \boldsymbol{\xi}_I)]} d^3x,$$

with the change of variables from $\boldsymbol{\xi}_I, \omega_I$ to $\boldsymbol{k}$ defined above.

Determination of incidence angle

When the input data is dominated by isolated specular reflection returns, the output will be dominated by such returns, as well. Asymptotically, in this case, the cascade of integrals is dominated by stationary phase contributions where the isochrons of the input and output travel times are tangent and share the same normal direction. This direction is also normal to the reflector at the specular point. When there is no mode conversion, at this specular point,

$$|\nabla_x \tau_I(\boldsymbol{x}, \boldsymbol{\xi}_I)| = \frac{2\cos\theta_I}{c(\boldsymbol{x})},$$

$$|\nabla_x \tau_O(\boldsymbol{x}, \boldsymbol{\xi}_O)| = \frac{2\cos\theta_O}{c(\boldsymbol{x})},$$

where $2\theta_I$ and $2\theta_O$ are the opening angles between the incident rays of the input and output source/receiver configurations at the point $\boldsymbol{x}$. Thus, we introduce two other KDM operators,

$$\cos_I = -\frac{1}{8\pi^3}\int |\nabla_x \tau_I(\boldsymbol{x}, \boldsymbol{\xi}_I)|(\cdots),$$

$$\cos_O = -\frac{1}{8\pi^3}\int |\nabla_x \tau_O(\boldsymbol{x}, \boldsymbol{\xi}_O)|(\cdots).$$

Here, $(\cdots)$ denotes the three lines of (10) beyond the integral sign. Then, the ratios of outputs,

$$\frac{\cos_I}{u_I(\boldsymbol{\xi}_O, \omega_O)}, \qquad \frac{\cos_O}{u_O(\boldsymbol{\xi}_O, \omega_O)},$$

will provide asymptotic estimates of θ_I and θ_O, respectively. These estimates of incidence angles provide the necessary additional tool for AVA analysis.

Frequency structure of the operator and asymptotic preliminaries.

We can anticipate an aspect of the asymptotic analysis from the form of result (10), alone. Two powers of frequency appear on the right side of this equation. The amplitude of 3D point source data has no power of frequency in its asymptotic (WKBJ) representation and the same should be true for the output. Each spatial integral carried out by stationary phase will produce an inverse

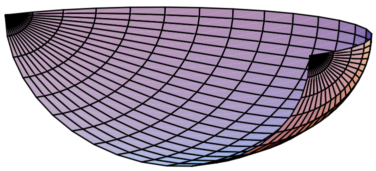

Figure 1. Example of an isochron surface: constant background, offset source and receiver. This isochron would arise in common offset or common shot source/receiver configurations.

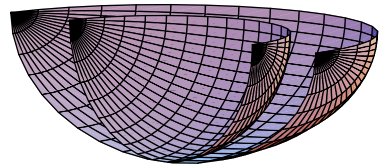

Figure 2. A point of tangency of isochrons from two travel time functions, corresponding to a simple stationary point in the integration over an isochron.

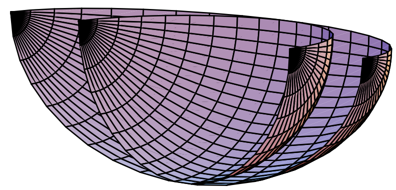

Figure 3. Tangency of isochrons along a curve of revolution.

power of the square root of frequency, if they are approximated by simple[§] stationary point contributions. There are five such integrations to be performed. Thus, *not all of the spatial integrals can be estimated by simple stationary point contributions* because the resulting power of ω on the two sides of the equation will not match. Clearly, then, some other method besides stationary phase must play a role in the analsysis of this integral.

It is in this context that Tygel, et al, [1998], employ a different approach. Consider the integral over the interior variables, represented by the differential, dV. Ultimately, this integral is recast as an integral over the isochrons of the input configuration, say, $\tau_I(\boldsymbol{x}, \boldsymbol{\xi}_O) = \text{constant} = t_I$, followed by integration over t_I. See Figure 1.

Suppose, for the moment, that the first two integrals are carried out by the method of stationary phase, with the last integral in the direction of increasing traveltime analyzed separately. In general, an isochron of τ_I is cut by the isochrons of τ_O. It is fairly straightforward to show that stationarity occurs when the normals of the two travel times line up; that is, the phase is stationary when *the isochron of* τ_O *is tangent to the isochron of* τ_I. Indeed, if there were a reflector at such a point with its normal being colinear with the normals to these two isochrons, then, on the data traces of the input and output data sets, there would be a specular return at the travel time evaluated on the input or output isochron and at the trace locations assigned to the input and output values of the parameters, $\boldsymbol{\xi}_I$ and $\boldsymbol{\xi}_O$, respectively.

Figure 2, depicts this tangency occurring at a single point. This corresponds to a simple stationary point in the integral over the isochron and the asymptotic order estimates proceed as described, above. However, in the simplest of situations, offset continuation and TZO/DMO in constant background, this is not what occurs! In such a medium, the isochrons are surfaces of revolution. They can be determined by taking the isochron in the vertical plane below the source and receiver and rotating about the line containing the source and receiver.

For this case, consider the mapping from input to output source/receiver configurations along parallel lines. It is easy to show that there are no stationary points unless the out-of-plane input and output variables are the same; $\xi_{I2} = \xi_{O2}$. Then, if the isochrons are tangent at a point, *they are tangent along the entire curve of revolution through that point*. See Figure 3. Thus, asymptotically, the ξ_{I2} integration behaves like a delta function and the integration in the direction of the generating curve of revolution of the isochron is an entire curve of stationarity. The order of the stationary point in this case is infinite and all orders of directional derivative of the phase in this direction vanish. This is a manifestation of a known fact about 3D DMO/TZO in constant background: while its kinematics are straightforward, its dynamics are not, and determination of amplitude dependence of the operator requires great care. This also should serve as a warning about 3D processing for the nonconstant background case. Suppose that the propagation speed(s) of the model are nearly constant. Then, formally, the straightforward multi-dimensional stationary phase described at the beginning of this section will seem to work. However, the second derivative in the direction of the curve of near-revolution will be small and the resulting amplitude will not be accurate for realistic frequencies of the exploration experiment. Thus, *uniform*

[§] A stationary point of a single integral is simple if the first derivative is zero, but the second derivative is not. In higher dimensions, all first derivatives are zero, but the matrix of second derivatives must have nonzero determinant.

asymptotic analysis is called for, if one is to obtain accurate amplitude information from the mapping process.

More generally, for the problem of offset continuation, a similar pathology occurs. If the offset difference is small, then the two isochrons are quite similar. Again, near total contact at stationarity will imply a small determinant of the matrix of second derivatives arising in the denominator of the stationary phase formula. In this case, the asymptotics breaks down and the predicted amplitude is not valid. For example, true amplitude offset continuation through small offsets cannot be achieved through the same process that produces TZO or its constant background equivalent, NMO/DMO. Here, the alternative method, Fomel [1995a,b, 1996, 1997] and Fomel et al [1996], for offset continuation is the method of choice.

2.5D KDM

Two-and-one-half (2.5D) processing is a technique for treating a single line of point source data in three dimensions. In this section, a KDM platform for processing such a single line of data is derived. First we develop the appropriate *thought experiment* from which to derive this 2.5D counterpart of (10). Consider a medium in which the propagation speed and other medium parameters are independent of one transverse direction, say x_2. It is further assumed that the input data is gathered on lines of constant x_2, say, $x_2 = \xi_{I2}$. Finally, consider an output source/receiver configuration that is also confined to lines of constant value of this out-of-plane coordinate. In this case, the input data is independent of the out-of-plane variable, namely, ξ_{I2}, and the integration in ξ_{I2} and in x_2 can be carried out by the method of stationary phase. Actually, it is easiest to first apply the stationary phase analysis in ξ_{I2} and then in x_2 as iterated integrals, rather than to do them together as a two-dimensional stationary phase calculation. The analysis has already been done in Bleistein, et al, [1997] and only the results will be reported here.

For the integration in ξ_{I2}, the phase to be considered is $\tau_I(\boldsymbol{x}, \boldsymbol{\xi}_I)$. The stationary point in ξ_{I2} is at $\xi_{I2} = x_2$ and the second component of the gradient of the phase is zero at this point. Furthermore,

$$\left.\frac{\partial^2 \tau_I}{\partial \xi_{I2}^2}\right|_{\xi_{I2}=x_2} = \frac{1}{\sigma_{Is}} + \frac{1}{\sigma_{Ig}} \tag{12}$$

In this equation, σ_{Is} (σ_{Ig}) is a running ray parameter along the ray from the source (receiver) to the scattering point, $\boldsymbol{x}$. It is the natural parameter that arises to describe out-of-plane geometrical spreading in the 2.5D case. It is related to travel time through the equation,

$$\frac{d\sigma}{d\tau} = c^2(\boldsymbol{x}), \tag{13}$$

with appropriate subscripts on both variables on the left. One can readily verify from this equation that σ has the dimensions of length^2/time. See Bleistein [1986] for further discussion.

When this value of ξ_{I2} is substituted into the phase, $\tau_I(\boldsymbol{x}, \boldsymbol{\xi}_I)$ is shown to be independent of x_2, making the second stationary phase analysis easier, since we only have to consider the phase, $\tau_O(\boldsymbol{x}, \boldsymbol{\xi}_O)$. The analysis on this phase proceeds exactly as described above. However, statationarity requires that $x_2 = \xi_{O2}$, essentially eliminating the out-of-plane coordinate from further consideration. All second component variables take on the same value.

Finally, the Beylkin determinant, (9), also becomes simpler in this case. It is given by

$$h(\boldsymbol{x}, \boldsymbol{\xi}_I) = \left[\frac{1}{\sigma_{Is}} + \frac{1}{\sigma_{Ig}}\right] H(\boldsymbol{x}, \xi_I), \tag{14}$$

with

$$H(\boldsymbol{x}, \xi_I) = \det \begin{bmatrix} \nabla_x \tau(\boldsymbol{x}, \xi_I) \\ \dfrac{\partial}{\partial \xi_I} \nabla_x \tau(\boldsymbol{x}, \xi_I) \end{bmatrix} \tag{15}$$

In this last equation, the gradient is a two component operator in (x_1, x_3) and ξ_I is a scalar variable.

Applying the method of stationary phase to the integral in (10) in both variables and taking account of the results stated above leads to the following 2.5D analog of that earlier result:

$$\begin{aligned} u_O(\xi_O, \omega_O) \sim \frac{\sqrt{|\omega_O|} e^{-i\pi \operatorname{sgn}(\omega_O)/4}}{4\pi^2} & \\ \cdot \int \sqrt{|\omega_I|} e^{i\pi \operatorname{sgn}(\omega_I)/4} d\omega_I d\xi_I & \\ \cdot \int u_I(\xi_I, \omega_I) \frac{a_O(\boldsymbol{x}, \xi_O)}{a_I(\boldsymbol{x}, \xi_I)} \frac{|\nabla_x \tau_O(\boldsymbol{x}, \xi_O)|}{|\nabla_x \tau_I(\boldsymbol{x}, \xi_I)|} & \\ \cdot \frac{\sqrt{\sigma_{Is} + \sigma_{Ig}}}{\sqrt{\sigma_{Os} + \sigma_{Og}}} \frac{\sqrt{\sigma_{Os}\sigma_{Og}}}{\sqrt{\sigma_{Is}\sigma_{Ig}}} |H(\boldsymbol{x}, \xi_I)| & \\ \cdot e^{[i\omega_O \tau_O(\boldsymbol{x}, \xi_O) - i\omega_I \tau_I(\boldsymbol{x}, \xi_I)]} d^2 x. & \end{aligned} \tag{16}$$

In this equation, we have rewritten ξ_I for ξ_{I1} and ξ_O for ξ_{O1}, since the second component is no longer in the representation and the formerly two component vectors are now scalars.

Equation (16) provides a platform for mapping data from any linear input source-receiver configuration and input medium parameters to data from a linear output source-receiver configuration and output medium parameters. It is a 2.5D transformation, meaning that it accounts for out-of-plane geometrical spreading but assumes modeling parameters that do not depend on the out-of-plane variable. We view it as a "platform," only, because it still requires an integration of the *operator* over the interior scattering variables. As above, for each choice of source/receiver configuration and medium parameters of input and output, this integral should be carried out in advance, preferably analytically, invoking asymptotic methods as appropriate. Then, for a given data set, one needs only to process the line of data by carrying out the integrals in the first line with the simplified weighting function obtained by the preprocessing analysis of the second and third lines. This is the usual form of TZO (NMO/DMO), for example.

Application of KDM to Kirchhoff data in 2.5D.

In this section, the application of the 2.5D KDM platform equation (16), to 2.5D Kirchhoff data is analyzed. That application leads to 2.5D Kirchhoff data, again, but with the input variables of the test data transformed to output variables. Had the derivation of (16) not used the obliquity approximation and had the reflection coefficient not been replaced by its stationary value, this could be argued to be a meaningless exercise. After all, the derivation started with the Kirchhoff model of the forward scattering problem. These extra approximations that were made along the way, however, make this a useful analysis, showing that these auxiliary approximations are valid within the context of the objective of our KDM, namely, to get the mapping of specular returns on the data trace correct!

To begin this analysis, define the reflector S_R through the curve,

$$\boldsymbol{x} = \boldsymbol{x}_R(\ell), \quad \boldsymbol{x} = (x_1, x_3). \tag{17}$$

Here, with no loss of generality, ℓ can be taken to be arclength along this curve which defines the reflector. The 2.5D Kirchhoff approximate data then has the representation [Bleistein, 1986]

$$\begin{aligned} u_I(\xi_I, \omega_I) = -\sqrt{|\omega_I|}e^{-i\pi\,\mathrm{sgn}\,(\omega_I)/4}F(\omega_I) \\ \int R(\boldsymbol{x}_R(\ell), \boldsymbol{x}_s(\xi_I)) \\ \cdot\hat{\boldsymbol{n}}_R \cdot \nabla_x \tau_I(\boldsymbol{x}_R(\ell), \xi_I) a_I(\boldsymbol{x}_R, \xi_I) \\ \cdot\frac{\sqrt{\sigma_{Is}(\boldsymbol{x}_R, \xi_I)\sigma_{Ig}(\boldsymbol{x}_R, \xi_I)}}{\sqrt{\sigma_{Is}(\boldsymbol{x}_R, \xi_I) + \sigma_{Ig}(\boldsymbol{x}_R, \xi_I)}} \\ \cdot e^{i\omega_I\tau_I(\boldsymbol{x}_R, \xi_I))]}d\ell. \end{aligned} \tag{18}$$

In this equation, $F(\omega_I)$ represents the source signature and $\hat{\boldsymbol{n}}_R$ is the upward unit normal on the reflector. Other expressions are defined as in earlier equations, except that now one of the points is $\boldsymbol{x}_R(\ell)$ on the reflecting surface.

This upward scattered field is inserted into (16). The result is

$$\begin{aligned} u_O(\boldsymbol{\xi}_O, \omega_O) &= -\sqrt{|\omega_O|}e^{-i\pi\,\mathrm{sgn}\,(\omega_O)/4} \\ &\quad \cdot\int |\omega_I| d\omega_I d\xi_I d\ell d^2x \mathcal{G} e^{i\Psi}. \end{aligned} \tag{19}$$

In this equation,

$$\Psi = \omega_O\tau_O(\boldsymbol{x}, \xi_O) - \omega_I\tau_I(\boldsymbol{x}, \xi_I) + \omega_I\tau_I(\boldsymbol{x}_R(\ell), \xi_I), \tag{20}$$

and

$$\begin{aligned} \mathcal{G} &= \frac{R(\boldsymbol{x}_R(\ell), \boldsymbol{x}_s(\xi_I))}{4\pi^2} \\ &\quad \cdot\hat{\boldsymbol{n}}_R \cdot \nabla_x \tau_I(\boldsymbol{x}_R(\ell), \xi_I) a_I(\boldsymbol{x}_R, \xi_I) \\ &\quad \cdot\frac{\sqrt{\sigma_{Is}(\boldsymbol{x}_R, \xi_I)\sigma_{Ig}(\boldsymbol{x}_R, \xi_I)}}{\sqrt{\sigma_{Is}(\boldsymbol{x}_R, \xi_I) + \sigma_{Ig}(\boldsymbol{x}_R, \xi_I)}} \\ &\quad \cdot\frac{a_O(\boldsymbol{x}, \xi_O)}{a_I(\boldsymbol{x}, \xi_I)} \frac{|\nabla_x \tau_O(\boldsymbol{x}, \xi_O)|}{|\nabla_x \tau_I(\boldsymbol{x}, \xi_I)|} \\ &\quad \cdot\frac{\sqrt{\sigma_{Is} + \sigma_{Ig}}}{\sqrt{\sigma_{Os} + \sigma_{Og}}} \frac{\sqrt{\sigma_{Os}\sigma_{Og}}}{\sqrt{\sigma_{Is}\sigma_{Ig}}} |H(\boldsymbol{x}, \xi_I)| \end{aligned} \tag{21}$$

is the cascade of the integrands of (18) and (16), exclusive of the explicit frequency dependence appearing here. In the last line, all σ's are functions of $\boldsymbol{x}$ rather than $\boldsymbol{x}_R$.

The method of stationary phase in the variable ℓ will be applied to this representation. The phase of interest is

$$\Phi_1(\ell) = \tau_I(\boldsymbol{x}_R(\ell), \xi_I) \tag{22}$$

To carry out the method of stationary phase, we need the derivatives,

$$\begin{aligned} \frac{\partial \Phi_1}{\partial \ell} &= \nabla_x \tau_I(\boldsymbol{x}_R, \xi_I) \cdot \frac{d\boldsymbol{x}_R}{d\ell}, \\ \frac{\partial^2 \Phi_1}{\partial \ell^2} &= \frac{\partial^2 \tau_R}{\partial x_{Ri}\partial x_{Rj}} \frac{dx_{Ri}}{d\ell}\frac{dx_{Rj}}{d\ell} + \frac{\partial \tau_R}{\partial x_{Ri}}\frac{d^2 x_{Ri}}{d\ell^2}. \end{aligned} \tag{23}$$

In these equations and those below, summation over the repeated indices, i, j, from 1 to 3, is to be understood. Setting the first derivative of Φ_1 equal to zero picks out the specular reflection point as the stationary point. Denote the stationary value of ℓ by $\overline{\ell} = \overline{\ell}(\xi_I)$. Detailed analysis of the second derivative is deferred for the moment. After stationary phase in ℓ, (19) becomes

$$
\begin{aligned}
u_O(\boldsymbol{\xi}_O, \omega_O) = -\sqrt{2\pi|\omega_O|}e^{-i\pi \operatorname{sgn}(\omega_O)/4} \\
\cdot \int \sqrt{|\omega_I|} F(\omega_I) e^{-i\pi \operatorname{sgn}(\omega_I \Phi_1'')/4} \\
\cdot d\omega_I d\xi_I d^2x \mathcal{G} \frac{e^{i\Psi}}{\sqrt{|\Phi_1''|}}, \\
\ell = \bar{\ell}(\xi_I).
\end{aligned}
\tag{24}
$$

Here, Φ_1'' denotes the value of the second derivative at the stationary point,

$$
\Phi_1'' = \left. \frac{\partial^2 \Phi(\ell)}{\partial \ell^2} \right|_{\ell=\bar{\ell}}, \tag{25}
$$

assumed to be nonzero. That is, the situation in which a caustic of the reflected wavefield is coincident with, or less than a "few" wavelengths from, the observation surface is excluded from consideration. However, the reflected rays may have passed through a caustic arising from the geometry of the surface, allowing Φ_1'' to be positive or negative. The case in which point source rays have caustics has been excluded, initially, by not including a KMAH index in our original Green's functions. Stationary phase in ξ_I is now to be appled to the integral in (24). The $\xi-$dependent part of the phase is

$$
\Phi_2 = \tau_I(\boldsymbol{x}_R(\bar{\ell}(\xi_I)), \xi_I) - \tau_I(\boldsymbol{x}, \xi_I). \tag{26}
$$

The derivatives of this expression with respect to ξ_I are given by

$$
\begin{aligned}
\frac{\partial \Phi_2}{\partial \xi_I} &= \frac{\partial \tau_I(\boldsymbol{x}_R(\bar{\ell}(\xi_I)), \xi_I)}{\partial \xi_I} - \frac{\partial \tau_I(\boldsymbol{x}, \xi_I)}{\partial \xi_I} \\
&\quad + \nabla_x \tau_I(\boldsymbol{x}_R(\bar{\ell}(\xi_I)), \xi_I) \cdot \frac{d\boldsymbol{x}_R}{d\bar{\ell}} \frac{d\bar{\ell}}{d\xi_I},
\end{aligned}
\tag{27}
$$

$$
\frac{\partial^2 \Phi_2}{\partial \xi_I^2} = \frac{\partial^2 \tau_I(\boldsymbol{x}_R(\bar{\ell}(\xi_I)), \xi_I)}{\partial \xi_I \partial x_{Rj}} \frac{d\boldsymbol{x}_{Rj}}{d\bar{\ell}} \frac{d\bar{\ell}}{d\xi_I} + \Delta\tau_I,
$$

where,

$$
\Delta\tau_I = \frac{\partial^2 \tau_I(\boldsymbol{x}_R(\bar{\ell}(\xi_I)), \xi_I)}{\partial \xi_I^2} - \frac{\partial^2 \tau_I(\boldsymbol{x}, \xi_I^2)}{\partial \xi_I^2}. \tag{28}
$$

In the first line in (27), the last term is zero because this is just the stationarity condition imposed on Φ_1. In the second line, summation over the repeated index, j, from 1 to 3 is understood.

Consider the condition that the first derivative of Φ_2 is equal to zero. The first travel time in Φ_2 is just the time for the specular ray path from source to S_R to the receiver. This travel time remains finite as ξ varies. On the other hand, the second term represents the travel time from the source to a fixed point at depth to a receiver. If the source/receiver array were of infinite extent, this travel time would increase beyond all bounds as the source/receiver pair moves off towards infinity in either direction. However, this travel time would achieve at least one local extremum (a minimum) at some finite value of ξ_I. Thus, the travel time difference will approach $-\infty$ at the extremes and reach some finite maximum for some value(s) ξ_I. If this ξ_I is in the range of integration, that is, in the range of source/receiver pairs for which data was collected, then the integral has a stationary point. If this ξ is not in the range, then, for that choice of $\boldsymbol{x}$, there is no stationary point and the contribution to the total integral is of lower order. We proceed as if there is an interior stationary point, $\xi_I = \xi_I(\boldsymbol{x})$.

Note that if $\boldsymbol{x}$ is on the reflector, then the ξ_I and $\bar{\ell}(\xi_I)$ for which this point is the specular reflection point satisfies both stationary phase conditions. An easy way to see this is to note that in this case, the rays from $\boldsymbol{x}$ and $\boldsymbol{x}_R$ to the source and receiver are the same and are specular. The fact that they are specular makes Φ_1 stationary; the fact that these two points are the same makes their derivatives with respect to ξ_I the same and the difference of derivatives appearing in $\partial\Phi_2/\partial\xi_I$ is then equal to zero. It is for this reason that the difference of second derivatives are combined into the expression $\Delta\tau_I$. This difference is equal to zero on the reflector and, therefore, near zero for $\boldsymbol{x}$ near the reflector. This will be important, below.

In order to determine the second derivative at stationarity, the first derivative of $\bar{\ell}$ with respect to ξ_I is needed. This derivative is determined by first setting $\partial\Phi_1/\partial\ell = 0$ in (23) and then differentiating implicitly with respect to ξ_I. This leads to the solution,

$$
\frac{d\bar{\ell}}{d\xi_I} = -\frac{\partial^2 \tau_I(\boldsymbol{x}_R(\bar{\ell}(\xi_I)), \xi_I)}{\partial \xi_I \partial x_{Rj}} \frac{dx_{Rj}}{d\ell} [\Phi_1'']^{-1}. \tag{29}
$$

With this result, (27) is replaced by

$$
\begin{aligned}
\frac{\partial^2 \Phi_2}{\partial \xi_I^2} &= \\
&- \left[\frac{\partial^2 \tau_I(\boldsymbol{x}_R(\bar{\ell}(\xi_I)), \xi_I)}{\partial \xi_I \partial x_{Rj}} \frac{d\boldsymbol{x}_{Rj}}{d\bar{\ell}} \frac{d\bar{\ell}}{d\xi_I} \right]^2 [\Phi_1'']^{-1} \\
&+ \Delta\tau_I.
\end{aligned}
\tag{30}
$$

The first factor on the right, here, can be simplified as follows.

$$
\begin{aligned}
\left| \frac{\partial^2 \tau_I(\boldsymbol{x}_R(\bar{\ell}(\xi_I)), \xi_I)}{\partial \xi_I \partial x_{Rj}} \frac{d\boldsymbol{x}_{Rj}}{d\bar{\ell}} \frac{d\bar{\ell}}{d\xi_I} \right| &= \left| \frac{\partial \nabla_x \tau_I}{\partial \xi_I} \cdot \frac{d\boldsymbol{x}_R}{d\bar{\ell}} \right| \\
&= \left| \frac{\partial \nabla_x \tau_I}{\partial \xi_I} \times \hat{\boldsymbol{n}}_R \right| \\
&= \frac{\left| \frac{\partial \nabla_x \tau_I}{\partial \xi_I} \times \nabla_x \tau_I \right|}{|\nabla_x \tau_I|}
\end{aligned}
\tag{31}
$$

$$= \frac{|H(\boldsymbol{x}_R,\xi_I)|}{|\nabla_x\tau_I|}.$$

In the second line, the two dimensional tangent to the reflector has been replaced by the two-dimensional normal to the reflector. In the next line, the colinearity (within a sign) of the surface normal and the traveltime gradient at stationarity is used. The last line, in turn, rewrites this two dimensional cross product as a determinant, the same Beylkin determinant as appears in the inversion formula. Howevr, it is now evaluated at the point, $\boldsymbol{x}_R$ on the reflector, subject to the two stationarity conditions, above. Now (30) can be rewritten as

$$\Phi_2'' = -\left|\frac{|H(\boldsymbol{x}_R,\xi_I)|}{|\nabla_x\tau_I|}\right|^2 [\Phi_1'']^{-1} + \Delta\tau_I. \tag{32}$$

As with Φ_1, the notation, Φ_2'', is introduced for the evaluation of the second derivative at the stationary point. We remark that for $\boldsymbol{x}$ near the reflector, this second derivative is dominated by the first term and

$$\operatorname{sgn}(\Phi_2'') = -\operatorname{sgn}(\Phi_1''),$$

while this sign might change "sufficiently far" from the reflector, presumably, more than three wavelengths away, for the sake of asymptotic analysis. The discussion of this possible latter region is postponed until later, and the analysis proceeds in the restricted range where the signs of the second derivate satisfy the stated relationship, above. In this case, application of the method of stationary phase to (24) leads to the result,

$$u_O(\boldsymbol{\xi}_O,\omega_O) = -2\pi\sqrt{|\omega_O|}e^{-i\pi\operatorname{sgn}(\omega_O)/4} \cdot\int F(\omega_I)d\omega_I d^2x\,\mathcal{G}\frac{e^{i\Psi}}{\sqrt{|\Phi_1''\Phi_2''|}}. \tag{33}$$

Here, the amplitude and the phase are to be evaluated at the dual stationary points in ℓ and ξ_I.

The dependence on ω_I has not become particularly simple. There is the linear dependence in Ψ, as defined by (20), and also the amplitude factor, $F(\omega_I)$. If $F=1$, the ω_I-integration yields a delta function. We take the point of view that F is a filter that leads to a bandlimited version of the delta function that we will denote by δ_B :

$$\delta_B(t) = \frac{1}{2\pi}\int F(\omega)e^{-i\omega t}d\omega. \tag{34}$$

By using this identity to carry out the ω_I integration in (33), we obtain

$$u_O(\boldsymbol{\xi}_O,\omega_O) = -4\pi^2\sqrt{|\omega_O|}e^{-i\pi\operatorname{sgn}(\omega_O)/4} \int d^2x\mathcal{G}\frac{e^{i\Psi}}{\sqrt{|\Phi_1''\Phi_2''|}} \cdot\delta_B(\tau_I(\boldsymbol{x}_R(\bar{\ell}),\xi_I)-\tau_I(\boldsymbol{x},\xi_I)). \tag{35}$$

The last factor here is a scalar delta function. Its argument is zero when $\boldsymbol{x}$ is on the reflector where the stationary conditions yield $\boldsymbol{x}=\boldsymbol{x}_R$ and the value of ξ_I makes the corresponding source/receiver pair specular. Furthermore, this zero is isolated; the gradient of the argument is just the gradient of the travel time, which is normal to the reflector. Thus, the direction of maximal change of argument of the delta function is initially normal to the reflector. Within a scale factor, then, this delta function is the *singular function of the surface*, S_R. The scale factor is just the magnitude of the gradient of the travel time, that is,

$$\delta_B(\tau_I(\boldsymbol{x}_R(\bar{\ell}),\xi_I)-\tau_I(\boldsymbol{x},\xi_I)) = |\delta(n_R)\nabla_x\tau_I(\boldsymbol{x}_R(\bar{\ell}),\xi_I)|. \tag{36}$$

Consequently, replacing the bandlimited delta function by the delta function, itself, (35) can be rewritten as

$$u_O(\boldsymbol{\xi}_O,\omega_O) = -4\pi^2\sqrt{|\omega_O|}e^{-i\pi\operatorname{sgn}(\omega_O)/4} \cdot\int d\ell\mathcal{G}\frac{e^{i\Psi}}{\sqrt{|\Phi_1''\Phi_2''|}|\nabla_x\tau_I(\boldsymbol{x}_R(\ell),\xi_I)|}. \tag{37}$$

In this equation, the stationarity conditions define $\xi_I=\xi_I(\ell)$, choosing the value of ξ_I for which the input source/receiver pair are specular at $\boldsymbol{x}_R(\ell)$. Now, the amplitude in this equation must be evaluated at stationarity and for $\boldsymbol{x}=\boldsymbol{x}_R$. In this limit, from (21),

$$\mathcal{G} = \frac{R(\boldsymbol{x}_R(\ell),\boldsymbol{x}_s(\xi_I))}{4\pi^2}a_O(\boldsymbol{x}_R,\xi_O) \hat{\boldsymbol{n}}_R\cdot\nabla_x\tau_I(\boldsymbol{x}_R(\ell),\xi_I)\frac{|\nabla_x\tau_O(\boldsymbol{x}_R,\xi_O)|}{|\nabla_x\tau_I(\boldsymbol{x}_R,\xi_I)|} \frac{\sqrt{\sigma_{Os}(\boldsymbol{x}_R,\xi_O)\sigma_{Og}(\boldsymbol{x}_R,\xi_O)}}{\sqrt{\sigma_{Os}(\boldsymbol{x}_R,\xi_O)+\sigma_{Og}(\boldsymbol{x}_R,\xi_O)}}|H(\boldsymbol{x},\xi_I)|. \tag{38}$$

Furthermore, the term, $\Delta\tau_I$, defined by (28), is zero and, from (32),

$$\sqrt{|\Phi_1''\Phi_2''|} = \frac{|H(\boldsymbol{x}_R,\xi_I)|}{|\nabla_x\tau_I|}. \tag{39}$$

These results are used in (37) to obtain

$$u_O(\boldsymbol{\xi}_O,\omega_O) = -\sqrt{|\omega_O|}e^{-i\pi\,\mathrm{sgn}\,(\omega_O)/4}$$
$$\cdot\int d\ell R(\boldsymbol{x}_R(\ell),\boldsymbol{x}_s(\xi_I))a_O(\boldsymbol{x}_R,\xi_O)$$
$$\cdot\hat{\boldsymbol{n}}_R\cdot\nabla_x\tau_I(\boldsymbol{x}_R(\ell),\xi_I)\frac{|\nabla_x\tau_O(\boldsymbol{x}_R,\xi_O)|}{|\nabla_x\tau_I(\boldsymbol{x}_R,\xi_I)|} \tag{40}$$
$$\cdot\frac{\sqrt{\sigma_{Os}(\boldsymbol{x}_R,\xi_O)\sigma_{Og}(\boldsymbol{x}_R,\xi_O)}}{\sqrt{\sigma_{Os}(\boldsymbol{x}_R,\xi_O)+\sigma_{Og}(\boldsymbol{x}_R,\xi_O)}}$$
$$e^{i\omega_O\tau_O(\boldsymbol{x}_R,\xi_O)}.$$

Since the integrand is evaluated subject to the stationarity relation between ℓ and ξ_I,

$$\hat{\boldsymbol{n}}_R\cdot\nabla_x\tau_I(\boldsymbol{x}_R(\ell),\xi_I) = -|\nabla_x\tau_I(\boldsymbol{x}_R,\xi_I)|. \tag{41}$$

Just as in (4), we set

$$|\nabla_x\tau_O(\boldsymbol{x}_R,\xi_O)| = -\hat{\boldsymbol{n}}_R\cdot\nabla_x\tau_O(\boldsymbol{x}_R(\ell),\xi_O). \tag{42}$$

With these substitutions,

$$u_O(\xi_O,\omega_O) = -\sqrt{|\omega_O|}e^{-i\pi\,\mathrm{sgn}\,(\omega_O)/4}$$
$$\cdot\int R(\boldsymbol{x}_R(\ell),\boldsymbol{x}_s(\xi_I))$$
$$\cdot\hat{\boldsymbol{n}}_R\cdot\nabla_x\tau_O(\boldsymbol{x}_R(\ell),\xi_O)a_O(\boldsymbol{x}_R,\xi_O) \tag{43}$$
$$\cdot\frac{\sqrt{\sigma_{Os}(\boldsymbol{x}_R,\xi_O)\sigma_{Og}(\boldsymbol{x}_R,\xi_O)}}{\sqrt{\sigma_{Os}(\boldsymbol{x}_R,\xi_O)+\sigma_{Og}(\boldsymbol{x}_R,\xi_O)}}$$
$$\cdot e^{i\omega_O\tau_O(\boldsymbol{x}_R,\xi_O))}d\ell.$$

The Kirchhoff representation in the input source/receiver coordinates has been transformed into the Kirchhoff representation in the output source/receiver coordinates. In obtaining this result, a region of the $\boldsymbol{x}$-domain where $\mathrm{sgn}\,(\Phi_2'') = \mathrm{sgn}\,(\Phi_1'') has been neglected.$ In this region, the delta function in time is replaced by a principal-value-$1/t$ function. This function also has its singular support centered around $t=0$. However, the $\boldsymbol{x}$-domain where this is the correct value for the signature is bounded away from $t=0$, which corresponded to the neighborhood of the reflector. Thus, any contribution that might be obtained from this combined integration over ω_I and $\boldsymbol{x}$ will be of lower order asymptotically than the result given here.

The source signature of the input data, $F(\omega_I)$ in (18), was used to define the bandlimited delta function that confined the $\boldsymbol{x}$-domain integration to the reflectiing surface. This, again, is a leading order asymptotic result. In another context, Tygel has suggested that such operators should be viewed as providing a "sinc-like" interpolation of the data in the neighborhood of the peak of the signal. This means an interpolation of the spatial part of the operator, appearing in lines two and three of (16), in the neighborhood of the reflector.

It is well known that the Kirchhoff integral provides the leading order asymptotic expansion of the return from specular reflections. Hence, travel time and all geometrical spreading and curvature effects, including effects of "buried foci," caustics produced by synclines, will be properly transformed by the KDM process. Where the caustic pierces the upper surface, the arrival time is expected to be accurate, but no claims are made about the accuracy of the amplitude. The factor, Φ_1'', is zero in this case and the asymptotic analysis is invalid. However, it produces an integrable singularity in the Kirchhoff integral, with the correct travel times in the phase, hence, our claim that the arrival time is correct, but the amplitude need not be.

For edge-diffracted returns, the Kirchhoff integral produces the correct arrival time, but an inaccurate diffraction coefficient, except at the shadow boundary of the last reflected ray. Thus, the mapped data is expected to contain mapped diffraction arrival times with inaccurate amplitudes.

There is another source of "error" in the amplitude. Note that the reflection coefficient is evaluated at an incidence angle associated with the input source/receiver configuration, through its dependence on the stationary value of ξ_I. For correctly mapped data, it would be preferable to have this dependence mapped to ξ_O. However, this is simply not the case. The input reflection coefficient is preserved, not mapped. This is known from the TZO case and is therefore not surprising in this general result.

In summary, we have shown that the leading order asymptotic input data is mapped to the leading order asymptotic output data, except for the reflection coefficient, which maintains its input value everywhere.

Conclusions

We have derived platforms for 3D and 2.5D KDM of scalar wavefields. The formalism assumes knowledge of a physical model for both the input and output data and prescribed input and output source/receiver configurations. By cascading an inversion formula with a modeling formula, we obtain the KDM platform formula. This cascade is a single reflector formalism in the absence of multiple reflections and multi-pathing. In that sense, it is still a somewhat limited result, at the level of generality of standard migration or DMOformalisms.

In the absence of a specific application, the formula includes a multifold integration over the physical model space that must be evaluated asymptotically for each example of KDM in order to derive a computationally feasible formalism for implementation. Application of this formalism in constant background 2.5D DMO produces the same formula as was derived in Bleistein, et al, [1998]. This is a straightforward exercise that is not included in this paper.

On the other hand, we show how Kirchhoff approximate model data in a given input configuration is mapped to Kirchhoff data in a different output configuration for the 2.5D case. We have done this in great generality, without specificying any particular configuration transformation. From this result, we conclude that the travel time and geometrical spreading effects of the input model are properly mapped to their counterparts in the output model, while the reflection coefficient is not.

In future papers, we will specialize the mapping platforms to achieve specific KDM formulas. Work is currently in progress on 3D constant background DMO and wave-equation-datuming.

Acknowledgment

The authors wish to acknowledge the critical reviews by John Stockwell and Steve Sheaffer. Their comments helped the authors signicificantly improve the exposition presented here.

References

Artley, C., and Hale, D., 1994, Dip moveout processing for depth-variable velocity: Geophysics, vol. 59, no. 4, pp. 610-622.

Berryhill, J. R., 1979, Wave field extrapolation techniques in seismic migration, a tutorial: Geophysics, 46, 1638-1656.

Bleistein, N., 1975, Direct Image Reconstruction of Anomalies in a Plane Via Physical Optics Far Field Inverse Scattering, J. Acoustical Soc. Amer., 59, 6.

Bleistein, N., 1976, Physical Optics Far Field Inverse Scattering in the Time Domain, J. Acoustical Soc. Amer., 60, 6.

Bleistein, N., 1986, Two-and-One-half dimensional inplane wave propagation: Geophysical Prospecting, 34, 686-703.

Bleistein, N., 1987, On the imaging of reflectors in the earth: Geophysics, 52, 7, 931-942.

Bleistein, N., and Cohen, J. K., 1979, The Singular Function of a Surface and Physical Optics Inverse Scattering: Wave Motion, 1.

Bleisten, N., J. K. Cohen and H. Jaramillo, 1997, True amplitude transformation to zero offset of data from curved reflectors: Geophysics, to appear.

Bleistein, N., Cohen, J. K., and Stockwell, J., 1998, Mathematics of Multi-Dimensional Seismic Inversion, Lecture notes, Center for Wave Phenomena.

Bojarski, N. N., 1967, Three dimensional short pulse inverse scattering: Spec. Proj. Lab. Rep., Syracuse University Res. Corp., Syracuse, N. Y.

Bojarski, N. N., 1968, Electormagnetic inverse scattering theory: Spec. Proj. Lab. Rep., Syracuse University Res. Corp., Syracuse, N. Y.

Bojarski, N. N., 1982, A survey of the physical optics inverse scattering identity: IEEE Trans. Ant. & Prop., AP-30, 980-989.

Biondi, B., and Chemingui, N., 1994, Transformation of 3-D prestack data by azimuthal moveiout: 64th Ann. Int. Mtg. SEG, Expanded Abstracts, 1541-1544.

Chen, W. and Stewart, R., 1996, Transformation of P-S to P-P seismic data: Crews Research Report, 8, 18-1, 18-25.

Cohen, J.K., Hagin, F.G., and Bleistein, N., 1986, Three-dimensional Born inversion with an arbitrary reference: Geophysics, 51, no. 8, 1552-1558.

Fomel, S., 1995a, Amplitude preserving offset continuation in theory, Part 1: the offset continuation equation: Stanford Exploratoin Project preprint, SEP-84, 179-196

Fomel, S., 1995b, Amplitude preserving offset continuation in theory, Part 2: solving the equation: Stanford Exploration Project preprint, SEP-89.

Fomel, S., 1997, Velocity continuation and the anatomy of prestack residual migration: 67th Annual International Meeting of the Society of Exploration Geophysicists, Expanded Abstracts, Vol II Tulsa, 1762-1765.

Fomel, S., N. Bleistein, H. Jaramillo, J. K. Cohen, 1996, True amplitude DMO, offset continuation and AVA/AVO for curved rreflectors: 66th Annual International Meeting of the Society of Exploration Geophysicists, Expanded Abstracts, Vol II, Tulsa, 1731-1734.

Gazdag, J. and Squazzero, P., 1984, Migration of seismic data by phase shift plus interpolation: Geophysics, 49, 124-131.

Hale, D., and C. Artley, 1993, Squeezing dip moveout for depth-variable velocity: Geophysics, 58, 2, 257-264.

Jaramillo, H. and Bleistein, N.,1997, A simplified derivation to migration and demigration in isotropic inhomogeneous media: Center for Wave Phenomena Annual Report, CWP-248, Geophysics, submitted.

Mager, R. D., and Bleistein, N., 1978, An Approach to the Limited Aperture Problem of Physical Optics Far Field Inverse Scattering: IEEE Trans. Ant. and Prop., AP-26.

Sheaffer, S., and Bleistein, N., 1998, 2.5D downward continuation using data mapping theory: Center for Wave Phenomena Research Report number

Tygel, M., Schleicher, J., and Hubral, P., 1995a, True-amplitude migration to zero offset (MZO) by diffraction stack: preprint Insitituto de Matemática Estatística e Ciência da Computação, Universidade Estadadual de Campinas, Brazil.

Tygel, M., Schleicher, J., and Hubral, P., 1995b, Dualities between reflectors and reflection time surfaces: Journal of Seismic Exploration, Vol. 4, pp. 123 - 150.

Tygel, M., Schleicher, J., Hubral, P., and Santos, L. T., 1998, 2.5-D true-amplitude Kirchhoff migration to zero offset in laterally inhomogeneous media: Geophysics, to appear.